

Analysis of Channel Estimation Error in Physical Layer Network Coding

Keyvan Yasami, Abolfazl Razi, and Ali Abedi, *Senior Member, IEEE*

Abstract—This article investigates the effect of erroneous channel estimation on performance of physical layer network coding over fading channels. In this scenario, the relay maps the superimposed noisy modulated data, received from the two end terminals, to network coded combination of the source packets. We consider channel estimation error to be Gaussian distributed and formulate the network coding error by the distance between real and estimated points in the channel coefficients plane. Using this model, we present a statistical lower bound on variance of estimation error that can be tolerated by the relay terminal without imposing a network coding error on the system.

Index Terms—Channel estimation error, physical layer network coding, cooperative relaying, network throughput.

I. INTRODUCTION

SINCE network coding was introduced [1], wireless network coding has received a lot of attention. This increased interest is due to considerable gains that can be achieved by application of network coding in wireless relaying scenarios. Physical layer network coding makes use of inherent additive nature of electromagnetic waves, arriving simultaneously at a relay, to further improve network coding and increase network throughput [2], [3].

Denoise-and-forward (DNF), a relaying scheme in which there is no need to decode the received signal at the relay, is introduced in [4], and later expanded in [5] to present adaptive network coding and modulation design. However the authors assume that relay terminal can accurately estimate the channel coefficients. The robustness of the DNF physical layer network coding scheme with respect to channel estimation error is studied in [6]. Channel estimation error is considered for both links and performance of this scheme, in terms of end-to-end network throughput, is evaluated for different values of estimation error. However, no analytical results are provided to calculate this performance degradation.

In this article, Gaussian error in channel estimation is considered, and a novel analytical method to determine a bound on tolerable error and hence performance of the network is proposed. This paper compliments our previous work [6] with an analytical lower bound on tolerable channel estimation error to avoid majority of network coding errors. The results presented in this article may be used as a design criterion for practical systems utilizing physical layer network coding.

Manuscript received February 11, 2011. The associate editor coordinating the review of this letter and approving it for publication was I. Maric.

This work is financially sponsored by the National Aeronautics and Space Administration (NASA) grant number EP-11-05-5404438.

The authors are with the Department of Electrical and Computer Engineering, University of Maine, Orono, ME, 04469 USA (e-mail: {keyvan.yasami, abolfazl.razi, ali.abedi}@maine.edu).

Digital Object Identifier 10.1109/LCOMM.2011.082011.110301

The rest of this paper is organized as follows. Section II describes the physical layer network coding and channel estimation parameters. Section III presents problem formulation and the proposed solution. Numerical and simulation results are presented in section IV. Section V concludes this paper.

II. SYSTEM MODEL

Consider a simple bidirectional relaying scenario, where terminal A and B have traffic to send to each other, and terminal R acts as a relay [5]. Terminal R performs maximum-likelihood (ML) detection, and quantizes the received signal from simultaneous transmission of data from A and B, i.e. $Y_R = H_A X_A + H_B X_B + Z_R$, using a denoising mapper C and a constellation mapper, \mathcal{M} , where H_A and H_B are the channel coefficients from terminals A and B to relay R, respectively; $Z_R \sim N(0, \sigma_n^2)$; X_A and X_B are the modulated symbols from terminals A and B.

The network coded data can be written as:

$$S_R = C(\hat{S}_A, \hat{S}_B), \quad (1)$$

where \hat{S}_A , and \hat{S}_B are ML estimates of digital data from A and B, namely S_A and S_B . Denoising maps are optimized by maximizing the minimum Euclidean distance between all transmitted signal pairs (S_A, S_B) and their estimates (\hat{S}_A, \hat{S}_B) [5].

The network code selection only depends on the channel amplitude ratio, γ , and phase difference, θ , i.e., [6]:

$$C = f(\gamma, \theta). \quad (2)$$

Note that $H_B/H_A = \gamma \exp(j\theta)$. It has been shown that erroneous channel estimation may lead to selection of a sub-optimum code, since the distance profile used for network code selection at the relay is based on the estimates of the channel coefficients and not the actual values [6]. Moreover, it has been shown that this non-optimal code selection may not lead to a network error if estimation errors are in a certain range. In this case, the network performance will not degrade drastically. In section III, we formulate impact of imperfect channel estimation on physical layer network coding to get a lower bound on this error range.

III. PROPOSED ANALYTIC SOLUTION

In this section, we assume Gaussian channel estimation error for both links A and B, i.e.,

$$\hat{H}_A = H_A + Z_1, \quad \hat{H}_B = H_B + Z_2, \quad (3)$$

where Z_1 and Z_2 are independent Gaussian random variables, $Z_1, Z_2 \sim N(0, \sigma^2)$. Relay node will use this erroneous data to perform network coding utilizing (2). The distance between

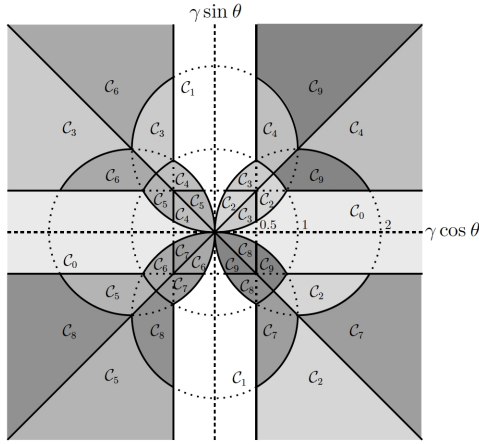


Fig. 1. Network Coding Map [5]. Each region is associated with a unique network code, C_i . For instance, note the symmetry between regions associated with codes C_0 and C_1 and between regions associated with codes C_2 to C_9 .

the Channel point $P_1 = (H_A, H_B)$ and the estimated point $P_2 = (\hat{H}_A, \hat{H}_B)$ in $H_A - H_B$ plane can be calculated using (3) as,

$$d_{P_1 P_2} = \sqrt{Z_1^2 + Z_2^2}. \quad (4)$$

Furthermore the network coding map consists of discrete region in the $\gamma - \theta$ plane according to (2). These regions, R_i , correspond to different network codes. Each region, R_i , may be represented by a statistical center, $P(x_c, y_c)$, with coordinates defined in $\gamma \cos \theta - \gamma \sin \theta$ plane as,

$$x_c = \mathbb{E}[x|R_i], \quad y_c = \mathbb{E}[y|R_i], \quad (5)$$

where $x = \gamma \cos \theta$ and $y = \gamma \sin \theta$, and $\mathbb{E}[\cdot]$ denotes expectation function.

The shortest distance between this point and any neighboring region is considered as an error threshold, T_i , for each region, R_i . If the points P_1 and P_2 are in different regions of the network coding map, then there will be a network error due to channel estimation error. At any region in $\gamma \cos \theta - \gamma \sin \theta$ plane, if the distance between the points P_1 and P_2 is greater than the corresponding threshold, i.e., $d_{P_1 P_2} \geq T_i$, or in terms of squared distance,

$$d_{P_1 P_2}^2 \geq T_i^2, \quad (6)$$

a network coding error will happen. To consider all points and regions, expected value of squared distance, $d_{P_1 P_2}^2$, and a weighted threshold of all regions should be considered, i.e.,

$$\mathbb{E}[d_{P_1 P_2}^2] \geq T^2, \quad (7)$$

where expectation is over the Gaussian random variables Z_1 and Z_2 and T^2 is the total weighted squared threshold defined as,

$$T^2 = \sum_i P_{R_i} T_i^2. \quad (8)$$

where P_{R_i} is the probability of region R_i . Substituting $d_{P_1 P_2}$ from (4) into (7), we have,

$$\sigma^2 \geq T^2/2, \quad (9)$$

which is lower bound on variance of estimation error, σ^2 , for which a network coding error will happen. Note that we have

TABLE I
PROBABILITY OF REGIONS IN NETWORK CODING MAP OF FIG. 1 FOR Rician CHANNEL EXAMPLE (K-FACTOR = 10 dB)

Region (R_i)	Probability (P_{R_i})
R_0 & R_1	0.2600
R_2 to R_9	0.0600

considered all the regions in calculating (9) to account for their probabilities.

Numerical solutions and simulations for this lower bound, under specific channel realizations, are presented in the next section.

IV. NUMERICAL RESULTS

In this section, a numerical value for the lower bound of (9) is derived. The proposed analytic solution in section III works regardless of the modulation scheme used at terminals A and B. However we assume QPSK modulation in this section for simplicity of our proposed solution. Although the proposed method may be applied to various channel models, in this article we used Rician model as an example. Probability distribution function (pdf) for both channels, H_A and H_B , is given by,

$$f(h|v, \sigma_r) = \frac{h}{\sigma_r^2} \exp\left(-\frac{(h^2 + v^2)}{2\sigma_r^2}\right) I_0\left(\frac{hv}{\sigma_r^2}\right), \quad (10)$$

where $I_0(\cdot)$ is modified zeroth order Bessel function of first kind, h is either H_A or H_B , with Rician K-factor (dB) = $10 \log_{10}(v^2/2\sigma_r^2)$.

For case of QPSK modulation at both terminals A and B and closest-neighbor clustering method the network code map (2) is presented in Fig. 1 [5]. As shown in this figure, 10 network codes are obtained in this case. The joint pdf of $\gamma \cos \theta$ and $\gamma \sin \theta$ can be calculated using (10),

$$f_{X,Y}(x, y) = \int_0^\infty \frac{w^3}{\sigma_r^4} \exp\left[\frac{(\gamma^2 + 1)w^2 + 2v^2}{2\sigma_r^2}\right] I_0\left(\frac{wv}{\sigma_r^2}\right) I_0\left(\frac{wv\gamma^2}{\sigma_r^2}\right) dw, \quad (11)$$

where $x = \gamma \cos \theta$, $y = \gamma \sin \theta$, and $\gamma^2 = x^2 + y^2$. (10) and (11) are used to generate numerical results in the following manner. Integrating (11) over each region, R_i , determines region probabilities. Table I demonstrates these probabilities for Rician channels with K-factor = 10 dB. Note that region R_0 and R_1 and regions R_2 to R_9 are symmetric as depicted in Fig. 1. Fig. 2 depicts regions R_0 and R_4 with their neighboring borders. R_0 and R_4 have 2 and 4 discrete sections, S_{ij} , respectively. The corresponding statistical centers, (x_c, y_c) , shortest distance to neighboring regions, T_{ij} , and section probabilities, $P_{S_{ij}}$, are given for all sections of each region in Table II.

By symmetry of the distributions and regions as shown in Fig. 1, R_1 has same thresholds as R_0 , and rest of regions have same thresholds as R_4 . Weighted threshold for each region can be defined as,

$$T_i = \sum_j P_{S_{ij}} T_{ij}. \quad (12)$$

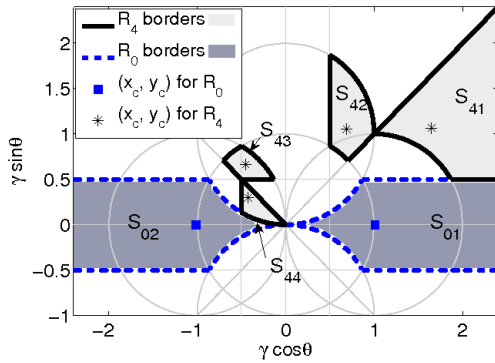


Fig. 2. Regions R_0 and R_4 with corresponding sections, borders, and statistical centers (x_c, y_c) . Sections and borders are given for any fading channel model, statistical centers are given for Rician channel example with K-factor = 10 dB.

Using (8), (12), values of P_{R_i} , $P_{S_{ij}}$, and T_{ij} , from Tables I and II, we have, $T^2 \approx 0.1$, and from (9),

$$\sigma \geq 0.22. \quad (13)$$

End-to-end network throughput in terms of number of delivered packets for different values of σ (standard deviation) are shown in Fig. 3. Note that packet error rate is used to evaluate the network throughput, since in practice, we cannot know which bit location has failed. We have applied cyclic redundancy check codes to packets to check whether one packet failed or succeeded.

In this simulation set, H_A and H_B are considered to be Rician distributed with previously mentioned parameters (K-factor = 10 dB). Packets of length 256 symbols are considered.

It is assumed that channel coefficients are constant during transmission of each packet. Signal to Noise Ratio (SNR) is defined as $(\mathbb{E}[|H_A|^2] + \mathbb{E}[|H_B|^2])/2\sigma_n^2$, where σ_n^2 is variance of zero mean additive Gaussian noise of channels. Moreover, to further concentrate on performance degradation due to network coding error, perfect ML detection is assumed at both end terminals, A and B, as well as relay, R.

Fig. 3 depicts end-to-end throughput for different values of σ (standard deviation) together with pure XOR network coding. In this figure, σ is increased by steps of size 0.04 from 0.14 to 0.30. A larger gap between curves corresponding to σ values of 0.22 and 0.26 is seen. This larger gap is due to network coding error, occurring for a larger quantity of symbols in comparison with number of network coding errors for smaller values of σ . The value of σ corresponding to this gap is between 0.22 and 0.26, which is in agreement with the lower bound given by (13). Also note that the performance curve for σ values greater than 0.22 are very close to the performance curve of XOR network coding, i.e., for these values of σ , there is no advantage in using 10 denoising maps at the relay than just the XOR network coding.

V. CONCLUSIONS

This article presents a statistical lower bound on variance (standard deviation) of channel estimation error to prevent network coding error, in a two way relaying system with physical layer network coding. Gaussian distributed error in estimation

TABLE II
STATISTICAL CENTERS, THRESHOLDS, AND SECTION PROBABILITIES OF REGIONS R_0 AND R_4 FOR RICIAN CHANNEL EXAMPLE (K-FACTOR = 10 dB)

Region (R_i)	Section (S_{ij})	Statistical Center (x_c, y_c)	Threshold (T_{ij}) (Shortest Distance)	Section Probability ($P_{S_{ij}}$)
R_0	S_{01}	(1.0090, 0)	0.4206	0.1300
	S_{02}	(-1.0090, 0)	0.4206	0.1300
R_4	S_{41}	(1.6479, 1.0658)	0.2472	0.0047
	S_{42}	(0.6899, 1.0522)	0.1899	0.0253
	S_{43}	(-0.4493, 0.6627)	0.1383	0.0253
	S_{44}	(-0.4260, 0.2947)	0.0740	0.0047

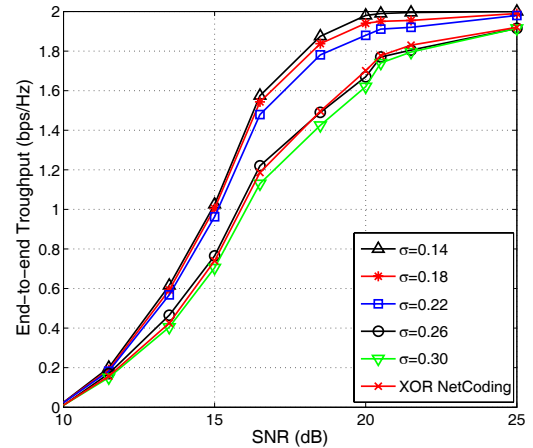


Fig. 3. End-to-end Network throughput (bps/Hz) vs SNR (dB) for different values of σ - Rician channel example with K-factor = 10 dB.

of channel coefficients is considered, and the network coding error event is formulated. Using the expected value of distance between real and estimated points in the channel coefficients plane, thresholds and statistical centers for different regions are defined as shown in Fig. 2. Utilizing region probabilities and thresholds, a lower bound on variance of estimation error is calculated. Although the proposed method may be applied to various channel models, in this article we used Rician model as an example. In case of Rician channels with K-factor = 10 dB, presented in Table II, the lower bound on standard deviation is calculated to be 0.22. Simulation results verified the analytically calculated lower bound on variance in terms of network throughput degradation.

REFERENCES

- [1] R. Ahlswede, N. Cai, S.-Y. R. Li, and R. W. Yeung, "Network information flow," *IEEE Trans. Inf. Theory*, vol. IT-46, pp. 1204–1216, July 2000.
- [2] S. Zhang, S. Liew, and P. Lam, "Physical layer network coding," in *Proc. ACM Mobicom*, pp. 358–365, Sep. 2006.
- [3] S. Katti, H. Rahul, W. Hu, D. Katabi, M. Medard, and J. Crowcroft, "XORs in the air: practical wireless network coding," *IEEE/ACM Trans. Networking*, vol. 16, pp. 497–510, June 2008.
- [4] P. Popovski and H. Yomo, "Bi-directional amplification of throughput in a wireless multi-hop network," in *Proc. VTC-Spring*, vol. 2, pp. 588–593, May 2006.
- [5] T. Koike-Akino, P. Popovski, and V. Tarokh, "Optimized constellations for two-way wireless relaying with physical network coding," *IEEE J. Sel. Areas Commun.*, vol. 27, pp. 773–787, June 2009.
- [6] K. Yasami and A. Abedi, "Effect of channel estimation error on performance of physical layer network coding," in *Proc. IEEE CCNC*, pp. 751–752, Jan. 2011.